ACS OMEGA

http://pubs.acs.org/journal/acsodf

Article

Parabolic Viscosity Behavior of NaCl-Thickened Surfactant Systems upon Temperature Change

Pengwei Jin,[⊥] Jun Wu,[⊥] Rongying Shi,* Li Dai, and Ying Li*

Cite This: *ACS Omega* 2023, 8, 37511−37520

Read Online

ACCESS | Metrics & More | Article Recommendations | Supporting Information

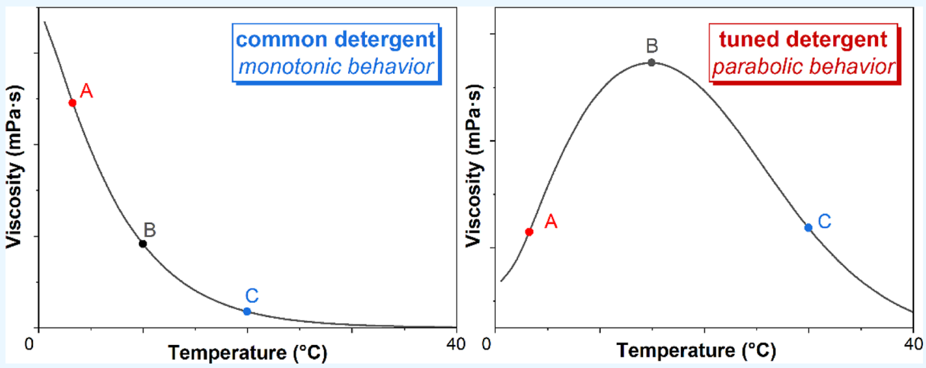

ABSTRACT: The viscosity of household care products plays an important role in pleasant delivery using consumer experience at home. A novel solution to mitigate the sharp rising of viscosities at low temperatures of detergents was proposed. By designing the formulation of the surfactant blend, formulators can achieve acceptable viscosity profiles in the temperature range encountered in daily life. The verification and modulation of formulas bearing parabolic viscosity−temperature behavior were systematically studied, including in single, binary, and ternary systems, based on the modulation of sodium ethoxylated alkyl sulfate (AES) by other anions, zwitterions, and nonions. The *R* ratio theory was used to have a better understanding of the molecular assembly of surfactants behind the parabolic behavior exhibited in rheology analyses. One of the key findings is that the parabolic viscosity−temperature phenomenon could be easily observed in the highly hydrated ethoxylated anionic systems like AES-based systems. For those anions lacking ethoxylation, especially sodium linear alkylbenzene sulfonate (LAS), the monotonic variation of hydration affinity with temperature led to the disappearance of parabola in the observed temperature window (>0 °C). Moreover, salinity played an important role in the hydration affinity of the polar group and the interaction between the hydrophilic headgroups. A balanced salinity should be optimized to modulate the hydration affinity in a desired range so that the parabola could be easily tuned within the target temperature region. These findings provide opportunities for the formulators in the household care industry to design products with better pourability through carefully selecting a combination of surfactants and fine-tuning their ratios to improve consumer use experience, especially in winter.

1. INTRODUCTION

Viscosity is an important parameter in home care products such as liquid laundry detergents and dishwashing detergents, as the viscosity of a formula determines the pourability of the product, which, in turn, contributes to consumer use experience. Market survey shows that the viscosities of most commercial products are designed in an appropriate range at room temperature for better pourability, which means that the liquid in the bottle needs neither long time to outflow nor short time for too much to come out. However, when the temperature decreases, the viscosities of many of them increase monotonically; some may show a sharp increase in the range of 0−10 °C (Figure 1), which results in difficulties in consumer application scenarios including pour out or squeeze out, especially in winter.

Thus, many attempts have been made in the industry to mitigate the increase in the viscosity of a fluid when cooling. As one of the common practices in the industry is to use NaCl as the thickener, one might consider reducing the level of NaCl in a product to mitigate the high-viscosity problem during winter. However, in this case, when the temperature goes back to room temperature in other seasons, the viscosity of the products drops quickly. Products may behave just like water in

Received: August 9, 2023
Accepted: September 14, 2023
Published: September 26, 2023

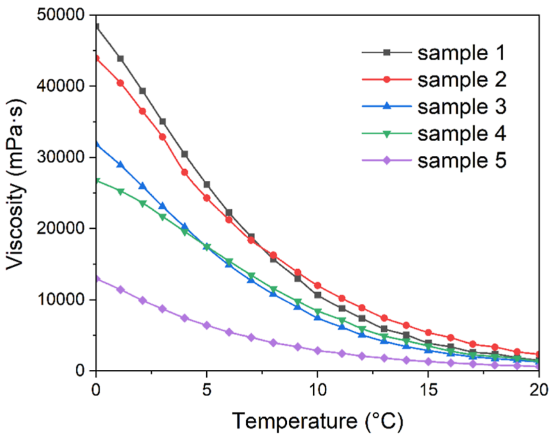

Figure 1. Viscosity changes of five representative commercial dishwashing detergents at different temperatures.

extreme conditions, making the user experience very unpleasant, and some consumers may question the level of the active content of the products in such conditions if a decent viscosity is intangible. Many formulators have tried other ways, such as addition of specific polymers[1] or formula adjustments. However, these methods cannot solve the high-viscosity problem fundamentally when the temperature decreases.

A deep understanding of colloidal theories may provide better solutions. In fact, the aggregation behaviors of surfactant molecules determine the phase structures of their solutions, which in turn control the viscosity and rheological properties of the systems.[2] The aggregation behaviors could be regulated by not only the concentration of surfactants but also the hydrophilic–lipophilic balance determined by the surfactant chemical structures and effected remarkably by temperature, salinity, etc., which shall provide practical solutions to address the viscosity problem.[3,4]

It has been reported that surfactant systems, especially the anionic ones, generally manifest a parabolic viscosity–temperature behavior.[5] This behavior can be utilized to modulate the viscosity profiles of home care products by a careful formulation design to achieve an ideal viscosity in which case the system goes through a stretched parabolic curve, resulting in an accepting viscosity profile in the low-temperature range, and the system would not go through a monotonic increase when the temperature decreases. For that purpose, existing colloidal theories such as negative interfacial tension in mixed films proposed by Schulman and Prince;[6] double-layer theory proposed by Schulman and Bowcott;[7] geometry arrangement theory proposed by Israelachvili, Mitchell, and Ninham;[8] and Winsor's R ratio of interaction between the interfacial layer and both phases[9] could all provide important directions. Among them, Winsor's R ratio theory provides a more comprehensive explanation that covers many factors, including concentration, temperature, salinity, etc., which will be used to guide our study reported in this paper.

Briefly, Winsor introduced the R ratio of the interaction energy between the surfactant and the oil phase vs the interaction energy between the surfactant and the aqueous phase to predict the phase behavior of the system. The modified definition of the R ratio is as follows (eq 1)[10,11]

$$R = \frac{A_{CO} - A_{OO} - A_{LL}}{A_{CW} - A_{WW} - A_{HH}} \tag{1}$$

where A_{CO} and A_{CW} indicate the interactions between the surfactant and oil and the surfactant and water, respectively. A_{OO} and A_{WW} indicate the interaction between oil and oil and water and water, respectively. A_{HH} and A_{LL} indicate the interactions between hydrophilic headgroups and hydrophobic tails. The value of R can be used to determine the curvature of the interface, in order to predict the phase behavior at the oil/water interface. When $R < 1$, the formation of O/W emulsion is preferred, while the formation of W/O emulsion is preferred when $R > 1$. Meanwhile, the lowest interfacial tension and maximum solubilization occur whenever $R = 1$, the formation of long-range-ordered aggregation systems, such as wormlike micelles, liquid crystals, or the bicontinuous phase, will also occur, depending on thermodynamic perturbation.

Although parabola-type formulas have been reported in some cases, gemini or cationic surfactants have to be used in these formulas, and the vertex of the parabola is located in the high-temperature region, higher than room temperature.[5,12−18] In the meantime, most of the rheological studies have focused on dilute system solution,[19] and only a few reports have studied the concentrated surfactant solution, which is close to the real applications.[20−22] It has been reported that, in a concentrated solution, a giant micelle including wormlike micelle will be formed, which is an important hotspot in surfactant studies due to its unique polymer-like behavior.[2,23−31] In dilute surfactant systems, the shape transition of micelles can be studied by static and dynamic light scattering,[32] while it is not feasible in a concentrated solution. Thus, the giant micelle for the latter has been studied by rheology, NMR, SANS, and visually FF-TEM or cryo-TEM.[33−37]

In this study, the verification and modulation of formulas bearing parabolic viscosity–temperature behavior were systematically studied, including in single, binary, and ternary systems. The distinction between the common monotonic system and the novel parabolic system was also further explained.

2. MATERIALS AND METHODS

2.1. Materials. Sodium linear alkylbenzene sulfonate (LAS) was obtained by neutralization of linear alkylbenzenesulfonic acid with NaOH. Linear alkylbenzenesulfonic acid (mainly C_{12}, average molecular weight 323), sodium ethoxylated alkyl sulfate (AES, 2EO, C_{12-14}, average molecular weight 383), coconut monoethanolamide (CMEA), coconut diethanolamide (CDEA), sodium fatty acid methyl ester sulfonate (MES), sodium dodecyl sulfate (SDS), and potassium laurate (LK) were obtained from Zhejiang Zanyu Technology Co., Ltd. Polyethoxylated fatty alcohols (AEO_3/AEO_7/AEO_9, C_{12-14}) were obtained from Anhui Jintong Fine Chemistry Co., Ltd. Sodium lauroyl glutamate (ULS-30S, ULS for short), sodium cocoyl alaninate (ACS-30S, ACS for short), sodium lauroyl sarcosinate (S-12), and potassium cocoyl glycinate (YCK-30K, YCK for short) were obtained from Nanjing Huashi New Material Co., Ltd. Sodium secondary alkanesulfonate (SAS), lauroylamidopropyl betaine (LAB), and alkyl polyglycosides (APG, C_{12-14}) were purchased from Clariant Chemicals (China) Ltd. Sodium glyceride ethoxylate sulfonate (SNS-80, SNS for short) was obtained from Sinolight Surfactants Technology Co., Ltd. Sodium fatty alcohol ether carboxylate (AEC, 9EO) was obtained from Jiangsu WanQi Biotechnology Co., Ltd. NaCl, NaOH, and sodium citrate were purchased from Shanghai Lingfeng Chemical Reagents Co., Ltd. Deionized water was prepared in the lab with a RO DI digital plus ultrapure water system from Hitech Instruments

https://doi.org/10.1021/acsomega.3c05855
ACS Omega 2023, 8, 37511−37520

Scheme 1. Representative Chemical Structures of Sodium Ethoxylated Alkyl Sulfate (AES, 2EO), Lauroylamidopropyl Betaine (LAB), and Sodium Linear Alkylbenzene Sulfonate (LAS)

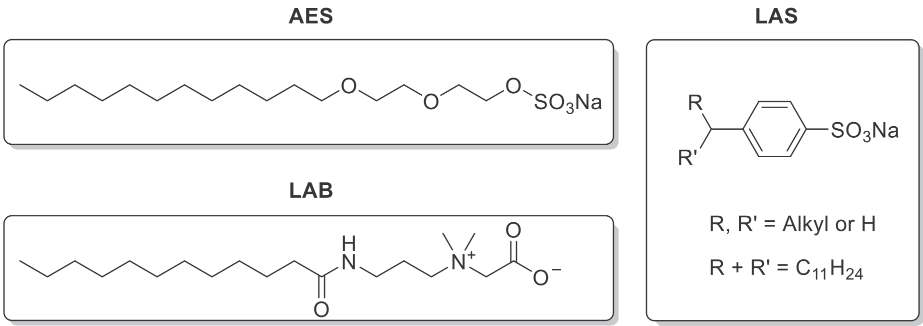

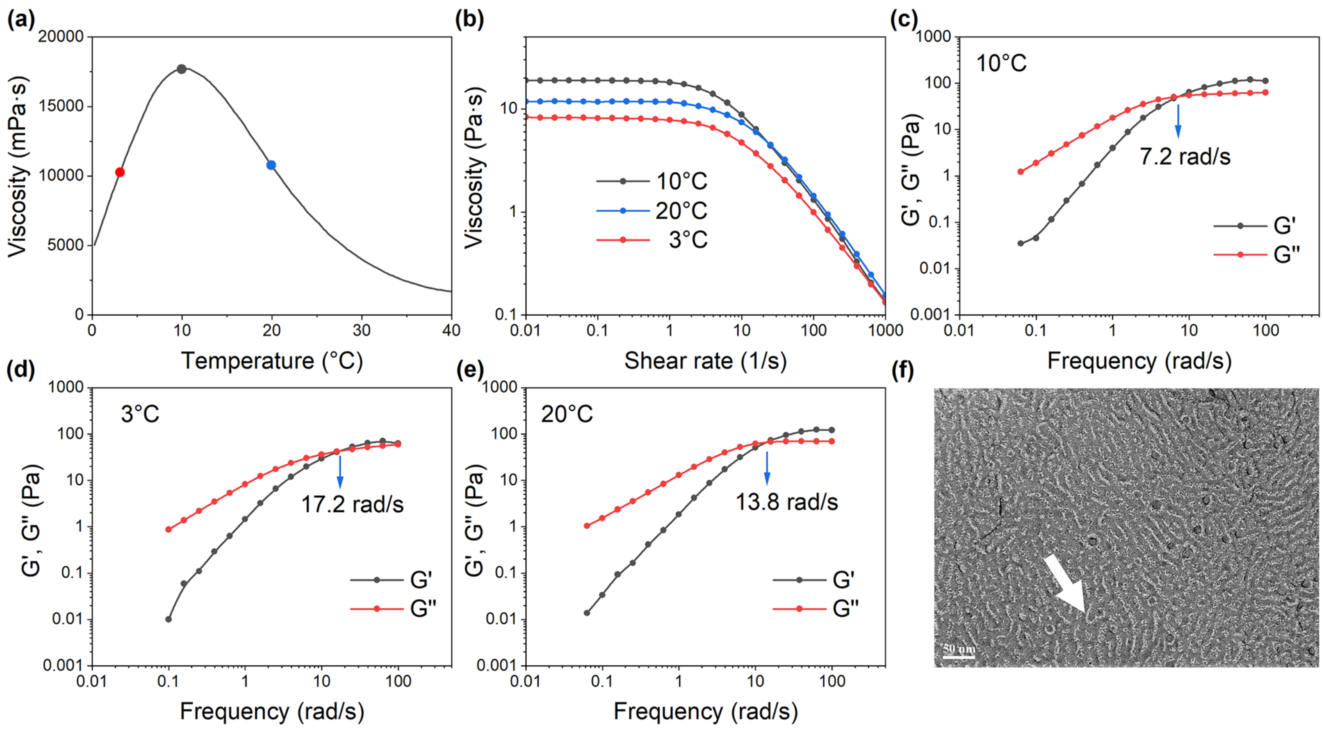

Figure 2. Temperature and rheological behaviors of AES (15% total active surfactant, pH 8.0, 3% NaCl). (a) Viscosity–temperature relationship. (b) Shear thinning effect at 3, 10, and 20 °C. (c–e) G' and G'' moduli at different temperatures. (f) FF-TEM image at 10 °C showing entangled wormlike micelles.

Co., Ltd. All the surfactants were of commercial grade, while the remaining materials were of analytical grade. Commercial products were purchased from a supermarket.

2.2. Sample Preparation. A mixture of surfactants was made by blending components in water with a total active surfactant concentration of 15 wt %. An IKA Eurostar 20 Digital mechanical stirrer was used for mixing at 300 rpm. The sample was kept at around 40 °C first to ensure sufficient dissolution using an IKA C-MAG HS 7 Control heater during blending. Afterward, the pH was adjusted carefully to 8.0 ± 0.1 (25 °C) using 10 wt % NaOH or sodium citrate solution with a METTLER TOLEDO FE28 pH meter. 1 wt % NaCl (unless otherwise stated) was added to thicken the system. Deionized water was added in the end to compensate for the evaporation loss. The sample was stirred homogeneously and stored in a 200 mL PET bottle sealed for 24 h prior to use.

2.3. Viscosity Measurement. Viscosity curves (0–25 °C) were recorded by a Brookfield DV3T LV viscometer equipped with a programmable thermostat bath (0–40 °C curves were recorded by the rheometer). Rheocalc T software was used to achieve automatic viscosity measurement using temperature profiles in a wide temperature range, and the cooling rate of the programmable thermostat was set at 7 min/°C. The temperature interval was set at 1.0 °C, and the measurement was conducted until the internal temperature of sample was within 0.1 °C of the set point. Spindle LV-62# or LV-63# was used. In addition, the entire measurement was run at a proper speed for 30 s according to the viscosity range of the sample to make torque in the 20–100% range as far as possible.

2.4. Rheological Measurement. Rheology was measured with a TA Instruments discovery HR-2 rheometer (a 60 mm parallel plate with Peltier plate aluminum, the gap was set around 500 μm). Frequency sweep (angular frequency 0.01–500 rad/s, 3, 10, 20 °C, or as-stated temperature, respectively. 1% strain in the linear viscoelastic region confirmed by the oscillation amplitude experiment), flow sweep (shear rate 0.01–1000 1/s, 3, 10, 20 °C, or as-stated temperature, respectively), and temperature ramp (0–40 °C, ramp rate 5

https://doi.org/10.1021/acsomega.3c05855
ACS Omega 2023, 8, 37511−37520

°C/min, shear rate 0.1 1/s, or as stated) were conducted to reveal the sample properties.

2.5. Freeze-Fracture TEM. The sample at a specific temperature was placed on a thin copper holder and then rapidly frozen in liquid nitrogen. The frozen sample was fractured in a freeze-fracture apparatus (Leica EM BAF 060, Germany). The replication was obtained by the deposition of platinum−carbon (Pt−C) and carbon.[38] The replicas were observed with a transmission electron microscope (JEOL Model JEM-2100).

3. RESULTS AND DISCUSSION

3.1. Verification of the AES System Bearing Parabolic Viscosity−Temperature Behavior. In this study, 15 wt % total active surfactant is selected and fixed, as the active matter both in laundry and in dishwashing detergents has been set by the industry as no less than 15 wt % in certain countries. Also, 1 wt % NaCl is fixed at first (otherwise stated) as viscosities resulting from it are in a suitable range compared to commercial products. The dosage of NaCl (less than the thickening critical) will not largely affect the position of the vertex in temperature−viscosity curves but effectively affect the magnitude of viscosity (Figure S1). Meantime, pH is set to 8.0 ± 0.1 (25 °C), which is a common practice as the mildness of the products at this condition is favored in laundry and dishwashing detergent industries. Another reason to fix the pH is to simplify the study as pH has a non-negligible influence on the temperature−viscosity curves (Figures S2 and S3). Representative surfactants mainly used in this study are depicted in Scheme 1. LAS and AES are largely used as commercial anionic surfactants in home care products due to their remarkable detergency and the high cost performance.[39] LAB is commonly used as a zwitterionic surfactant both in home care and in personal care products due to its mildness and thickening effect.[40]

Our initial study started from a simple surfactant system, which contained only one anionic surfactant, AES, and water. To have an easier measurement, 3% NaCl is added as the thickener to have a better viscosity profile.[38] As predicted by Winsor's R ratio theory, the system manifests a parabolic viscosity−temperature behavior (Figure 2a). The vertex of the parabola can be found at 10 °C with 17,700 mPa·s. Be aware that the shear rate is 0.1 1/s, which is slow enough to yield a linear behavior (Newtonian plateau) of the viscosity. One of the key measures in this work is to take a viscosity test every 1 °C interval to ensure the precise depicture of the parabolic behavior of the system.

Further rheological studies were carried out. 3, 10, and 20 °C on the simple AES system were chosen as the representative temperatures, which cover both high- and low-viscosity areas of the system. The flow sweeps for AES at varying temperatures are depicted in Figure 2b. All the lines showed Newtonian behavior at a low shear rate, the while shear thinning effect occurred obviously at high shear rate. The inflection points of curves (intersection of tangents, determination demonstrated in Figure S7) were located around 6.3, 9.5, and 10 1/s shear rate at 10, 3, and 20 °C, respectively. The higher the viscosity, the lower the shear rate of the inflection point. With increasing shear rate exceeding a critical point, chainlike structures will orient orderly, leading to a decrease of the viscosity. The more the degree of orientation, the lower the viscosity.[41] The frequency sweeps under different temperatures (Figure 2c−e) demonstrated that the crossover between elastic modulus G' and viscous modulus G'' at 10 °C was at lower frequency (7.2 rad/s) than that at 20 °C (13.8 rad/s) and 3 °C (17.2 rad/s). It has been indicated that the lower frequency of crossover means easy formation of a wormlike micelle and a network structure with a longer relaxation time.[22,42−44] Increased micellar length leads to an increase in zero-shear viscosity, whereas branching and network formation are proposed to lower the zero-shear viscosity.[45] Thus, the result suggested that at 10 °C, wormlike micelles formed, and the viscosity was higher, while at 3 and 20 °C, the wormlike micelles may branch or transform to rod-like micelles, resulting in the decrease of viscosity. It is worth mentioning that to obtain a qualified flow sweep experiment, a small gap should be used to suppress secondary flow (turbulence and eddy current), and equilibration time should be extended to reach the steady state in the low shear rate regime to avoid the false appearance of "shear-thickening" phenomena. In all experiments, samples should be carefully transferred to the rheometer to avoid small bubbles.

In order to confirm the formation of wormlike micelles, freeze-fracture TEM (FF-TEM) was conducted on the AES system at 10 °C, where the viscosity was relatively high. Clearly, wormlike micelles can be observed (Figure 2f, black), and a dark dot may be the end caps of the wormlike micelles (one of the end caps is pointed out with the white arrow in the image).

Actually, the parabolic viscosity−temperature behavior could be explained according to Winsor's R ratio theory. In the above AES system, the aggregation system was mainly influenced by the interactions between the hydrophilic headgroup and water (A_{CW}) and between the hydrophilic headgroups (A_{HH}). As there was no oil phase and the interaction between hydrophobic tails (A_{LL}) influenced by salinity and temperature was negligible, A_{CO}, A_{OO}, and A_{LL} in the numerator of the R ratio (eq 1) could be treated as constants. Keep in mind that the interaction energy in the R ratio is negative for attraction and positive for repulsion. The following description of the interaction energy is only for its absolute value.

AES has a higher hydration affinity due to the sulfate group and two or three ethoxy groups, which could be easily influenced by temperature. However, to have a stronger hydration affinity, a higher temperature is preferred for anionic groups, while a lower temperature is preferred for ethoxylated groups. At low temperature (for instance, 3 °C), a smaller R ratio was calculated, which was dominated by the strong interaction between the hydrophilic headgroup and water (A_{CW}). When the temperature rose to around 10 °C, the interaction between the hydrophilic headgroup and water (A_{CW}) dropped to some extent due to the reduction of the hydrogen bonding of the ethoxy groups, which resulted in a big R ratio approaching 1, where a wormlike micelle was formed due to the suitable molecular geometry. The increase of the contour length of the wormlike micelle resulted the highest viscosity. With the increase in the temperature (above 20 °C), the interaction between the hydrophilic headgroup and water (A_{CW}) dropped again due to the intense molecular thermal motion. However, the repulsion between the hydrophilic headgroups (A_{HH}) and that between water (A_{WW}) increased intensively, which covered the decrease of A_{CW} and led to a lower value of the R ratio (be aware that A_{CO} and A_{CW} are negative values). The reduction of the average contour chain length or the transformation to the branched ones of wormlike

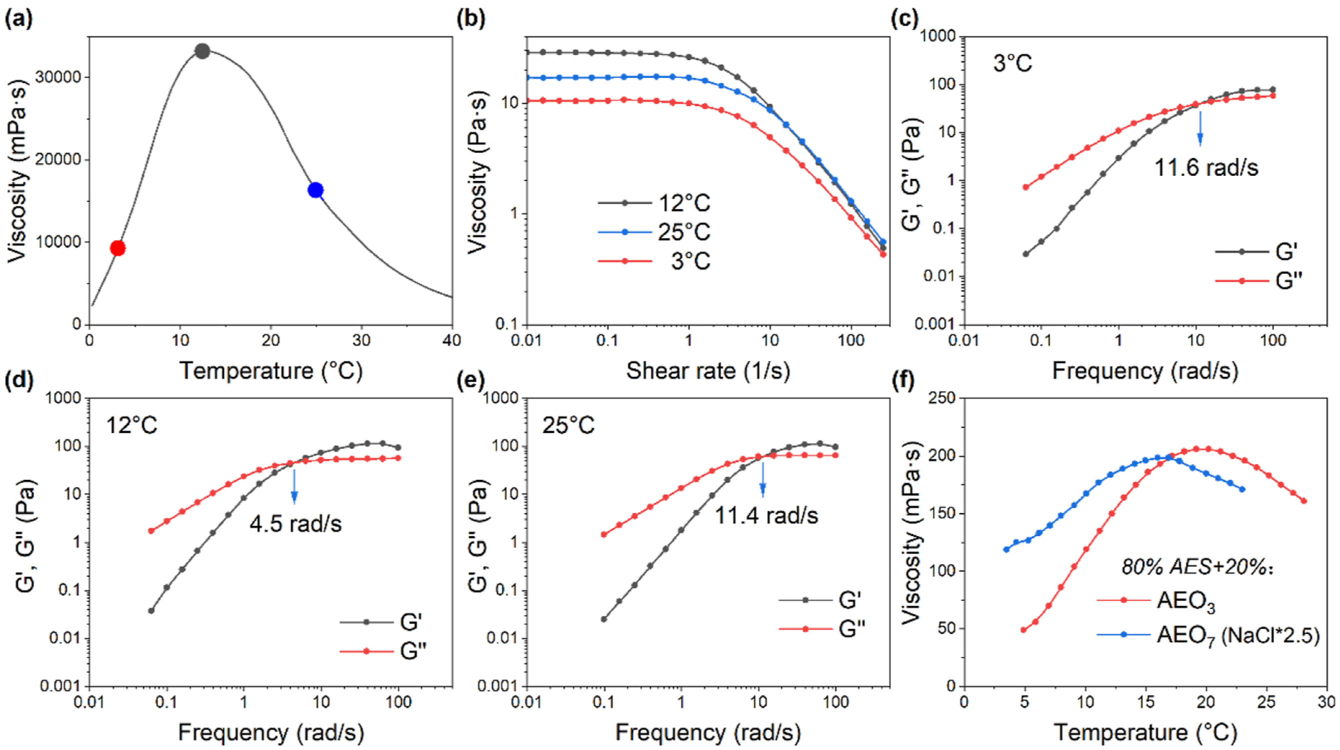

Figure 3. Temperature and rheological behaviors of 80% AES + 20% LAB (15% total active surfactant, pH 8.0, 1% NaCl). (a) Viscosity–temperature relationship. (b) Shear thinning effect at 3, 12, and 25 °C. (c–e) G' and G'' moduli at different temperatures. (f) Viscosity–temperature relationship of 80% AES + 20% AEO_3/AEO_7 (15% total active surfactant, 1%/2.5% NaCl).

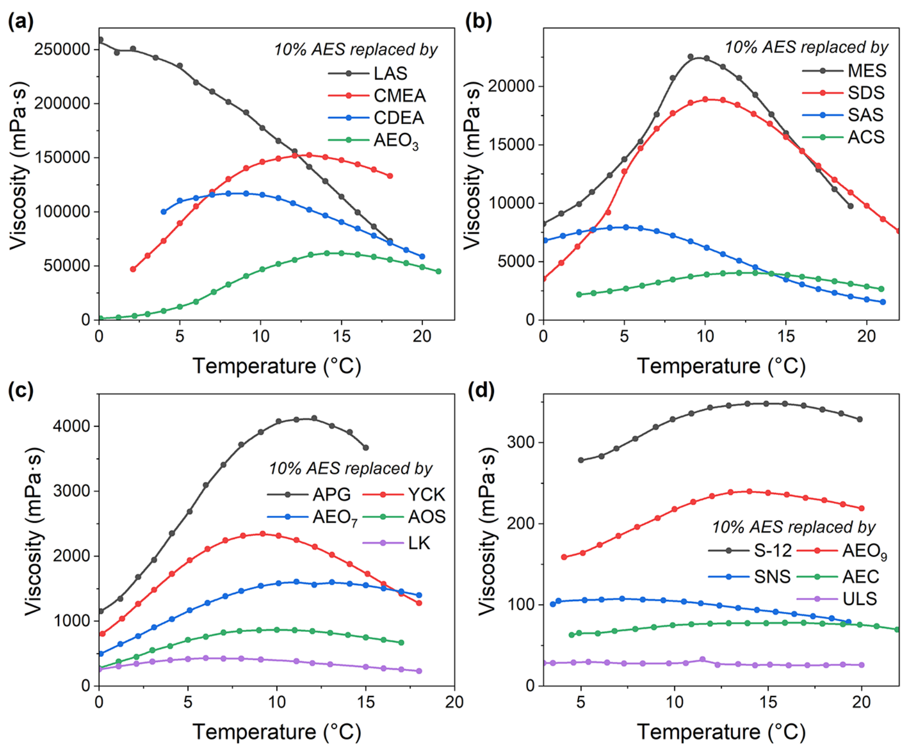

Figure 4. Viscosity–temperature relationship of 20% LAB + 70% AES + 10% replace surfactant (15% total active surfactant, pH 8.0, 1% NaCl). (a–d) Curves in different viscosity regions.

micelles resulted in the decrease of viscosity. Thus, a parabolic viscosity–temperature behavior is demonstrated.

3.2. Parabolic Viscosity–Temperature Behavior in AES/X Binary Systems.

Considering that the synergy of surfactants is vital in real applications, cleaning products are often binary or ternary systems. Since only an anionic surfactant could be thickened effectively by salt, it is vital to have at least one anionic surfactant in the combination of

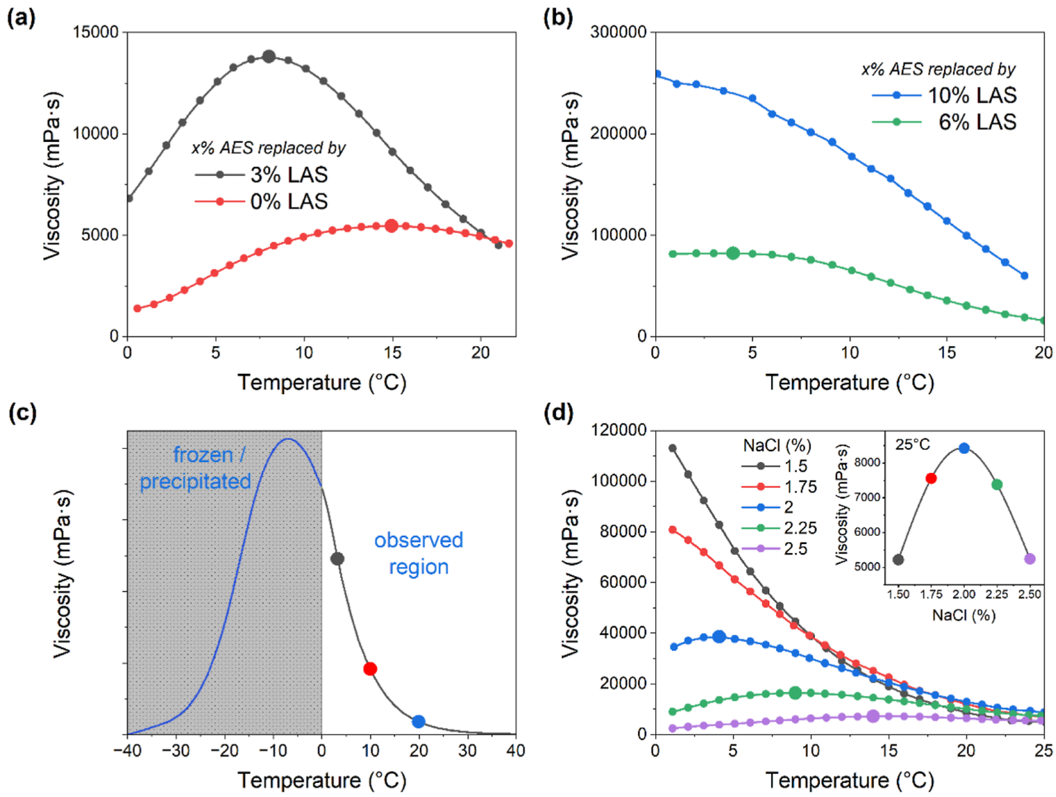

Figure 5. (a,b) Viscosity−temperature relationship of 80% AES + 20% LAB (15% total active surfactant, pH 8.0, and 1% NaCl) with AES partially replaced by LAS. (c) Possible explanation of monotonical viscosity behavior. (d) Viscosities of 60% AES + 40% LAS (15% total active surfactant, pH 8.0) along with temperature change. Inset shows the viscosity−NaCl relationship at 25 °C.

anionic, nonionic, and zwitterionic surfactant. A further study demonstrated that the parabolic viscosity−temperature behavior could be observed in the system of AES + zwitterionic and AES + nonionic mixed-surfactant systems.

In the beginning, a typical binary system bearing anionic and zwitterionic surfactants was studied. It was demonstrated that 80% AES + 20% LAB (for clarity, all the surfactant systems were in weight ratio out of 15 wt % total active surfactant) using 1 wt % NaCl (for clarity, all NaCl is in weight ratio of the whole system) as a thickener showed a near-symmetrical parabola (Figure 3a). (The influence of pH and NaCl on the parabolic curve is depicted in Figures S1−S3.) The vertex of the parabola can be found at 12 °C with 33,000 mPa·s, which is much easier to thicken than AES alone (AES used 3% NaCl). The inflection points of curves (intersection of tangents) are located around 3.2, 5.5, and 6.0 1/s shear rate at 12, 25, and 3 °C, respectively (Figure 3b). At 12 °C, the crossover between G' and G'' was at lower frequency (4.5 rad/s) than that at 25 °C (11.4 rad/s) and 3 °C (11.6 rad/s) (Figure 3c−e), which indicated that the high viscosity may be related to the wormlike micelle formation at 12 °C, while at 3 and 25 °C, the wormlike micelles may branch or transform to rod-like micelles, resulting in the decrease of viscosity.

In addition, the anionic and nonionic binary systems were also verified (Figure 3f). It was demonstrated that 80% AES + 20% AEO_3 showed a parabola and vertex that can be found at 20 °C with only 200 mPa·s. A similar system using AEO_7 needs 2.5-fold NaCl to keep the same viscosity level. This means that the anionic and nonionic binary system also has the parabolic behavior, except that the viscosity is quite low, which is in accordance with our common knowledge that nonions are difficult to thicken by salt. Similar to the single AES system, the aggregation in the AES/X binary system was mainly influenced by the interactions between the hydrophilic headgroup and water (A_{CW}) and between the hydrophilic headgroups (A_{HH}). With the increase of the temperature, the R ratio rose first and then dropped, resulting in a parabolic viscosity−temperature behavior.

3.3. Parabolic Viscosity−Temperature Behavior in AES/LAB/Y Ternary Systems. After the binary system was verified, it was intriguing to know how other surfactants (the ternary system) would influence the curve. To start conservatively, 10% AES was replaced by a third surfactant, meaning 80% AES + 20% LAB system becomes 70% AES + 20% LAB + 10% third one, which can be common anions and nonions, with other conditions remained the same (Figure 4, 15 wt % total active surfactant, pH 8.0, 1 wt % NaCl). The results demonstrated that various surfactants may result in different viscosity responses. Partial replacement of AES by LAS, CMEA, CDEA, and AEO_3 caused significant viscosity enhancement, which can be higher than 50,000 mPa·s (Figure 4a). Partial replacement of AES by MES, SDS, SAS, and ACS also caused considerable viscosity enhancement, ranging from 4000 to 23,000 mPa·s (Figure 4b). On the other hand, partial replacement of AES by APG, YCK, AEO_7, AOS, and LK caused viscosity to decrease lower than 4500 mPa·s (Figure 4c). In addition, the partial replacement by S-12, AEO_9, SNS, AEC, and ULS caused viscosity to decrease considerably, which can be lower than 300 mPa·s (Figure 4d). Here, ULS is the most difficult amino acid-based surfactant to be thickened due to its "big head", the hydrophilic moiety, that leads to a low packing parameter,[46] especially in alkaline condition.

https://doi.org/10.1021/acsomega.3c05855
ACS Omega 2023, 8, 37511−37520

Actually, the thickening issue of the amino acid-based surfactant is a hotspot in the industry.[40,43,47−49] Among these replacements, most curves retained the parabolic behavior, although the vertex temperature varied within the 5−15 °C range. This offers multiple possibilities to modulate the formula.

However, there was one exception. When 10% AES was replaced with 10% LAS, the parabola disappeared, showing a monotonic increase with cooling. This is an interesting phenomenon that only 10% AES replacement by LAS caused the type change of the viscosity−temperature curve, which was studied in detail in the next section.

Similarly, the rheology of the ternary systems was studied (Figures S4 and S5). Nonion APG and anion ACS applied systems were chosen as representatives due to the comparable viscosities similar to the single and binary system. For the 20% LAB + 70% AES + 10% APG system, the inflection points of curves (intersection of tangents) are located around 4.8, 8.1, and 9.1 1/s shear rate at 10, 3, and 20 °C, respectively (Figure S4a). At 10 °C, the crossover between G' and G'' was at lower frequency (8.4 rad/s) than that at 3 °C (23.5 rad/s) and 20 °C (19.0 rad/s) (Figure S4b−d). The 20% LAB + 70% AES + 10% ACS system shares a similar result. The inflection points of curves (intersection of tangents) are located around 2.5, 2.7, and 3.3 1/s shear rate at 10, 3, and 20 °C, respectively (Figure S5a). At 10 °C, the crossovers between G' and G'' was at lower frequency (4.4 rad/s) than that at 3 °C (5.0 rad/s) and 30 °C (7.5 rad/s) (Figure S5b−d). Similar to the single AES system and the AES/X binary system, the aggregation in the AES/LAB/Y ternary system was mainly influenced by the interactions between the hydrophilic headgroup and water (A_{CW}) and between the hydrophilic headgroups (A_{HH}). Although the third Y components have quite different influences on viscosity, generally R ratio still rose first and then dropped with the increase of the temperature, resulting in a parabolic viscosity−temperature behavior (except for LAS).

3.4. Understanding about the Exceptional Behavior of LAS. Previously, 10% AES replacement by LAS caused a type change in the viscosity-temperature curve (Figure 4a), which might hint that 10% replacement was too much and had exceeded the critical point. Consequently, 3 and 6% replacement of AES by LAS was further tested (Figure 5a,b). It was delightful to find that the parabola remained when 3% AES was replaced by LAS, and the parabola almost disappeared when 6% AES was replaced by LAS. Along with the LAS composition increase (ranging from 0, 3, 6, to 10%), the viscosity increased dramatically, and the vertex shifted to a lower temperature (ranging from 15, 8, 4 °C, to below 0 °C). It was believed that the parabola did not disappear, but just the vertex shifted to a lower temperature below 0 °C, in which the samples are frozen or the surfactant precipitated, thus showing a monotonical behavior in the observed region (Figure 5c).

It was clear that the rheological properties of LAS-dominated systems were unlike those of the other parabolic systems. As LAS is massively used in the home care field, despite that LAS originated from petroleum and should be reduced in the future, investigating whether the fixed dosage of NaCl (1%) influenced the usage of LAS in the parabolic system would be meaningful. The rheological properties of a LAS-dominated system (50% LAS + 50% AES, 15% total active surfactant, pH 8.0, and 1% NaCl) with respect to the temperature (Figure S6a) was first examined. The inflection points of curves (intersection of tangents) were located around 5, 15, and 80 1/s shear rate at 3, 10, and 20 °C, respectively. The shear-thinning effect is much obvious at 3 °C, while it remains the Newtonian fluid in a wide frequency domain at 20 °C. The high viscosity observed in the Newtonian plateau can be interpreted as the result of the presence of an entangled network of wormlike micelles. The frequency of the crossover between G' and G'' showed a positive relationship with temperature increase (105.1, 19.2, and 7.7 rad/s at 20, 10, and 3 °C, respectively) (Figure S6b−d), indicating that the wormlike micelles may transform to branched ones or the reduction of the average contour chain length of wormlike micelles, resulting in the decrease of viscosity, as the system goes through temperature increase from 3 to 20 °C.

In a word, if the vertex of the parabola is desired to be modulated to a proper temperature higher than 0 °C, certain restrictions need to be applied, especially the less use of LAS. The outstanding thickening effect of LAS by NaCl should be attributed to its unique molecular structure (Scheme 1). First, LAS is one of the few surfactants bearing the benzene ring, which may form the $\pi-\pi$ stack easily compacted by NaCl. Secondarily, industrial LAS is a mixture. The benzene ring can be connected to position 1−6 of the linear dodecane (normally very few in position 1), and the alkyl chain of LAS is branched. (Be aware that the word "linear" means that the starting material alkanes are linear, not the final molecules linear). Thus, the large lipophilic moiety makes LAS easier in the micelle formation with high viscosity.

The vertex shift of the parabola toward the lower temperature along with the dosage increase of LAS could also be explained according to Winsor's R ratio theory. Similar to the explanation for the AES system mentioned earlier, the criteria of the inflection point of the parabola was the competition of the interaction energies between A_{CW} and the sum of A_{WW} and A_{HH}. For LAS, A_{CW} is relatively smaller than that of AES as LAS has a poorer hydration affinity than AES, but the $\pi-\pi$ stack of the benzene rings of LAS leads to a higher A_{HH} than that of AES, which causes the turning of the parabola at a lower temperature with a higher LAS ratio.

Then, a simple and commonly used AES/LAS binary system (60% AES + 40% LAS, 15% total active surfactant, and pH 8.0) was established, and the dosage influence of NaCl was studied (Figure 5d). As is well known to all formulators, along the increase of NaCl in a simple anion-based surfactant system, the viscosity will increase first to a maximum value, where a lamellar/wormlike/hexagonal/cubic micelle/liquid crystal or conjugate phase may form. However, viscosity drops when NaCl exceeds a certain amount, which is believed that the collapse of the micelle network structure and the decrease of hydration ability lead to the decrease of the viscosity. As demonstrated in Figure 5d inset, the thickening effect reached the highest when the dosage of NaCl is 2%. When viscosity−temperature curves with various NaCl were recorded (Figure 5d), monotonic curves were found when NaCl was 1.5 and 1.75% as expected, but surprisingly, the parabola appeared when NaCl was ≥2%. Meantime, with the dosage of NaCl increased gradually from 2, 2.25, to 2.5%, the vertex of the parabola shifted accordingly to a higher temperature from 4, 9, to 14 °C, respectively. This is a helpful finding that LAS will not need to be restricted within a small portion when a parabola curve of viscosity−temperature is preferred, as long as the formula be tuned carefully, including the combination of surfactants and the proper dosage of NaCl. However, it is worth mentioning that too much salt is unfavored in the

https://doi.org/10.1021/acsomega.3c05855
ACS Omega 2023, 8, 37511−37520

commercial products, as precipitation or opaqueness may occur at low temperature.

The viscosity decrease caused by the excessive NaCl has been revealed extensively and is well known by formulators. However, the vertex shift of the parabola toward the higher temperature along with the dosage increase of NaCl is complicated. The excessive NaCl does not contribute to the viscosity increase but just helps the collapse of the micelle network structure or even the precipitation of the surfactant. The excessive NaCl consumes too much water leading to a decrease of hydration ability within molecules; thus, a relatively higher temperature will be needed to have a higher R ratio approaching 1, which would have a highest viscosity.

3.5. Mechanism Understanding of the Parabolic Viscosity–Temperature Phenomenon. Through the exploration of AES-based single, binary, and ternary systems, including the exceptional LAS and the over dosage of NaCl, it could be determined that the parabolic viscosity–temperature phenomenon of surfactant composite systems could provide an approach to adjust the rheological properties, of which the nature needs to be understood clearly. As discussed in Section 3.1, the main reason which led to the parabolic behavior of AES solution was the competition between A_{CW} and A_{HH} in the denominator of the R ratio equation, while A_{CW} was dominated by the hydration affinity which would be influenced tremendously by temperature. Although the hydration affinity of the anionic group increases along with temperature rises, a decrease occurs intensively with the ethoxylated group. Thus, the parabolic viscosity–temperature phenomenon could be easily observed in the highly hydrated ethoxylated anionic systems like AES-based systems, where the hydration affinity with temperature has an opposite variation between the anionic group and ethoxylated group. For those anions lacking ethoxylation, especially LAS, the monotonic variation of hydration affinity with temperature led to the disappearance of parabola in the observed temperature window (>0 °C). The $\pi-\pi$ stack of the benzene rings in LAS made the situation much subtle. In a word, if a parabolic viscosity–temperature curve is preferred, more anions with higher hydration affinity should be used.

On the other hand, the hydration affinity of the polar group A_{CW} and the interaction between the hydrophilic headgroups A_{HH} is highly affected by salt, and a proper salinity should be optimized to modulate the hydration affinity in a desired range, where the parabolic curve could be easily generated along with the temperature change.

4. CONCLUSIONS

In summary, the parabola viscosity–temperature behavior of diverse surfactant composition systems thickened by NaCl was systematically studied, including in single, binary, and ternary systems based on the modulation of AES by other anions, zwitterions, and nonions. The R ratio theory was applied to have a better understanding of the molecular assembly of surfactants behind the parabolic behavior exhibited in rheology analyses. One of the key findings is that the parabolic viscosity–temperature phenomenon could be easily observed in the highly hydrated ethoxylated anionic systems like AES-based systems. For those anions lacking ethoxylation, especially LAS, the monotonic variation of hydration affinity with temperature led to the disappearance of parabola in the observed temperature window (>0 °C). Moreover, salinity played an important role in the hydration affinity of the polar group and the interaction between the hydrophilic headgroups. A balanced salinity should be optimized to modulate the hydration affinity in a desired range, so that the parabola could be easily tuned within the target temperature region. The findings provide opportunities for the formulators in the home care industry to carefully select a combination of surfactants and fine-tune their ratios in the products, so that the product with better pourability can be developed to improve consumer use experience, especially in winter.

ASSOCIATED CONTENT

Supporting Information

The Supporting Information is available free of charge on the ACS Publications Web site. The Supporting Information is available free of charge at https://pubs.acs.org/doi/10.1021/acsomega.3c05855.

Influence of NaCl/pH on the parabolic curve; rheological behaviors of ternary systems (AES + LAB + APG/ACS), and typical system in the industry (AES + LAS) (PDF)

AUTHOR INFORMATION

Corresponding Authors

Rongying Shi – *Shanghai Hutchison WhiteCat Co., Ltd., Shanghai 200231, P. R. China*; Email: lucky.shi@whitecat.com

Ying Li – *Key Laboratory of Colloid and Interface Chemistry of State Education Ministry, Shandong University, Jinan, Shandong 250100, P. R. China*; orcid.org/0000-0002-2862-083X; Email: yingli@sdu.edu.cn

Authors

Pengwei Jin – *Shanghai Hutchison WhiteCat Co., Ltd., Shanghai 200231, P. R. China*; orcid.org/0000-0001-7090-680X

Jun Wu – *Zhejiang Wansheng Co., Ltd., Zhejiang 317000, P. R. China*

Li Dai – *Nanjing Huashi New Material Co., Ltd., Nanjing 210009, P. R. China*

Complete contact information is available at: https://pubs.acs.org/10.1021/acsomega.3c05855

Author Contributions

⊥P.J. and J.W. contributed equally to this work.

Notes

The authors declare no competing financial interest.

ACKNOWLEDGMENTS

The authors thank the Shanghai Rising-Star Program (20QB1402900) and the National Science Fund of China (nos. 21872084 and 61575109) for providing financial support to this project.

REFERENCES

(1) Huancao, W.; Shichao, T.; Huadai, L. YES thickening agent used in liquid washing products. *Deterg. Cosmet.* **2009**, *32*, 27–29.

(2) Ji, X.; Tian, M.; Wang, Y. Temperature-Induced Aggregate Transitions in Mixtures of Cationic Ammonium Gemini Surfactant with Anionic Glutamic Acid Surfactant in Aqueous Solution. *Langmuir* **2016**, *32*, 972–981.

(3) Singh, A.; Chaturvedi, K. R.; Sharma, T. Natural surfactant for sustainable carbon utilization in cleaner production of fossil fuels:

Extraction, characterization and application studies. *J. Environ. Chem. Eng.* **2021**, *9*, 106231.
(4) Singh, A.; Sharma, T.; Kumar, R. S.; Arif, M. Biosurfactant Derived from Fenugreek Seeds and Its Impact on Wettability Alteration, Oil Recovery, and Effluent Treatment of a Rock System of Mixed Composition. *Energy Fuels* **2023**, *37*, 6683−6696.
(5) Feng, Y.; Chu, Z.; Dreiss, C. A.; Thermo-responsive Wormlike Micelles. *Smart Wormlike Micelles*; SpringerBriefs in Molecular Science: Springer, Berlin, Heidelberg, 2015.
(6) Schulman, J. H.; Stoeckenius, W.; Prince, L. M. Mechanism of Formation and Structure of Micro Emulsions by Electron Microscopy. *J. Phys. Chem. A* **1959**, *63*, 1677−1680.
(7) Bowcott, J. E.; Schulman, J. H. Emulsions Control of droplet size and phase continuity in transparent oil-water dispersions stabilized with soap and alcohol. *Z. Elektrochem.* **1955**, *59*, 238−290.
(8) Israelachvili, J. N.; Mitchell, D. J.; Ninham, B. W. Theory of self-assembly of hydrocarbon amphiphiles into micelles and bilayers. *J. Chem. Soc., Faraday Trans. 2* **1976**, *72*, 1525−1568.
(9) Winsor, P. A. Hydrotropy, solubilisation and related emulsification processes. *Trans. Faraday Soc.* **1948**, *44*, 376−398.
(10) Uchiyama, H.; Acosta, E.; Tran, S.; Sabatini, D. A.; Harwell, J. H. Supersolubilization in Chlorinated Hydrocarbon Microemulsions: Solubilization Enhancement by Lipophilic and Hydrophilic Linkers. *Ind. Eng. Chem. Res.* **2000**, *39*, 2704−2708.
(11) Bourrel, M.; Chambu, C. The Rules for Achieving High Solubilization of Brine and Oil by Amphiphilic Molecules. *Soc. Pet. Eng. J.* **1983**, *23*, 327−338.
(12) Du, X.; Li, L.; Lu, Y.; Yang, Z. Unusual viscosity behavior of a kind of anionic gemini surfactant. *Colloids Surf., A* **2007**, *308*, 147−149.
(13) Kalur, G. C.; Frounfelker, B. D.; Cipriano, B. H.; Norman, A. I.; Raghavan, S. R. Viscosity Increase with Temperature in Cationic Surfactant Solutions Due to the Growth of Wormlike Micelles. *Langmuir* **2005**, *21*, 10998−11004.
(14) Tobita, K.; Sakai, H.; Kondo, Y.; Yoshino, N.; Kamogawa, K.; Momozawa, N.; Abe, M. Temperature-Induced Critical Phenomenon of Hybrid Surfactant As Revealed by Viscosity Measurements. *Langmuir* **1998**, *14*, 4753−4757.
(15) Wang, B.; Liu, L.; Zheng, C.; Lu, H. pH and temperature-responsive wormlike micelles formed by single amine oxide surfactant. *J. Dispersion Sci. Technol.* **2018**, *39*, 539−547.
(16) Xu, N.; Wei, J.; Kawaguchi, Y. Rheology Test on Shear Viscosity of Surfactant Solution: Characteristic Time, Hysteresis Phenomenon, and Fitting Equation. *Ind. Eng. Chem. Res.* **2016**, *55*, 5817−5824.
(17) Tam, K. C.; Wu, X. Y.; Pelton, R. H. Poly(N-isopropylacrylamide). II. Effect of polymer concentration, temperature, and surfactant on the viscosity of aqueous solutions. *J. Polym. Sci., Part A: Polym. Chem.* **1993**, *31*, 963−969.
(18) Ma, Y.; Heil, C.; Nagy, G.; Heller, W. T.; An, Y.; Jayaraman, A.; Bharti, B. Synergistic Role of Temperature and Salinity in Aggregation of Nonionic Surfactant-Coated Silica Nanoparticles. *Langmuir* **2023**, *39*, 5917−5928.
(19) Acharya, D. P.; Varade, D.; Aramaki, K. Effect of temperature on the rheology of wormlike micelles in a mixed surfactant system. *J. Colloid Interface Sci.* **2007**, *315*, 330−336.
(20) Parker, A.; Fieber, W. Viscoelasticity of anionic wormlike micelles: effects of ionic strength and small hydrophobic molecules. *Soft Matter* **2013**, *9*, 1203−1213.
(21) Vu, T.; Koenig, P.; Cochran, B. M.; Ananthapadmanabhan, K. P.; Weaver, M.; Reeder, B.; Hutton, H. D.; Kasting, G. B. Thickening mechanisms for an amino acid-derived surfactant composition. *Colloids Surf., A* **2020**, *589*, 124424.
(22) Vu, T.; Weaver, M. R.; Kasting, G. B.; Koenig, P. Effect of pH on the Structure and Dynamics of Wormlike Micelles in an Amino Acid-Derived Surfactant Composition. *Langmuir* **2021**, *37*, 4112−4120.
(23) Wei, X.; Geng, P.; Han, C.; Guo, Y.; Chen, X.; Zhang, J.; Zhang, Y.; Sun, D.; Zhou, S. Rheological Properties of Viscoelastic Solutions in a Cationic Surfactant-Organic Salts-Water System. *Ind. Eng. Chem. Res.* **2016**, *55*, 5556−5564.
(24) Kaler, E. W.; Zana, R. *Giant Micelles: Properties and Applications*; CRC Press: Boca Raton, 2007.
(25) Cates, M. E.; Candau, S. J. Statics and dynamics of worm-like surfactant micelles. *J. Phys. Condens. Matter* **1990**, *2*, 6869−6892.
(26) Holmberg, K.; Jönsson, B.; Kronberg, B.; Lindman, B. *Surfactants and Polymers in Aqueous Solution*; 2 nd Ed.; John Wiley & Sons: New York, 2002.
(27) Shrestha, R. G.; Shrestha, L. K.; Aramaki, K. Formation of wormlike micelle in a mixed amino-acid based anionic surfactant and cationic surfactant systems. *J. Colloid Interface Sci.* **2007**, *311*, 276−284.
(28) Zhang, Y.; Han, Y.; Chu, Z.; He, S.; Zhang, J.; Feng, Y. Thermally induced structural transitions from fluids to hydrogels with pH-switchable anionic wormlike micelles. *J. Colloid Interface Sci.* **2013**, *394*, 319−328.
(29) Morita, C.; Imura, Y.; Ogawa, T.; Kurata, H.; Kawai, T. Thermal-Sensitive Viscosity Transition of Elongated Micelles Induced by Breaking Intermolecular Hydrogen Bonding of Amide Groups. *Langmuir* **2013**, *29*, 5450−5456.
(30) Zou, W.; Larson, R. G. A mesoscopic simulation method for predicting the rheology of semi-dilute wormlike micellar solutions. *J. Rheol.* **2014**, *58*, 681−721.
(31) Ginzburg, V. V. Mesoscale Modeling of Micellization and Adsorption of Surfactants and Surfactant-Like Polymers in Solution: Challenges and Opportunities. *Ind. Eng. Chem. Res.* **2022**, *61*, 15473−15487.
(32) Christov, N. C.; Denkov, N. D.; Kralchevsky, P. A.; Ananthapadmanabhan, K. P.; Lips, A. Synergistic Sphere-to-Rod Micelle Transition in Mixed Solutions of Sodium Dodecyl Sulfate and Cocoamidopropyl Betaine. *Langmuir* **2004**, *20*, 565−571.
(33) Lu, S.; Wu, J.; Somasundaran, P. Micellar evolution in mixed nonionic/anionic surfactant systems. *J. Colloid Interface Sci.* **2012**, *367*, 272−279.
(34) Lu, S.; Somasundaran, P. Coexistence and Growth of Micellar Species in a Sugar-Based Surfactant/Phenol Mixture Studied by Analytical Ultracentrifugation. *Langmuir* **2007**, *23*, 9188−9194.
(35) McCoy, T. M.; Valiakhmetova, A.; Pottage, M. J.; Garvey, C. J.; Campo, L. D.; Rehm, C.; Kuryashov, D. A.; Tabor, R. F. Structural Evolution of Wormlike Micellar Fluids Formed by Erucyl Amidopropyl Betaine with Oil, Salts, and Surfactants. *Langmuir* **2016**, *32*, 12423−12433.
(36) Reilly, T.; Mohamed, M. I. H.; Lehmann, T. E.; Alvarado, V. Amphiphilic second-order phase transitions determined through NMR. *J. Mol. Liq.* **2018**, *268*, 647−657.
(37) Zou, W.; Tan, G.; Jiang, H.; Vogtt, K.; Weaver, M.; Koenig, P.; Beaucage, G.; Larson, R. G. From well-entangled to partially-entangled wormlike micelles. *Soft Matter* **2019**, *15*, 642−655.
(38) Mu, J.; Li, G.; Jia, X.; Wang, H.; Zhang, G. Rheological Properties and Microstructures of Anionic Micellar Solutions in the Presence of Different Inorganic Salts. *J. Phys. Chem. B* **2002**, *106*, 11685−11693.
(39) Li, H.; Dang, L.; Yang, S.; Li, J.; Wei, H. The study of phase behavior and rheological properties of lyotropic liquid crystals in the LAS/AES/H2O system. *Colloids Surf., A* **2016**, *495*, 221−228.
(40) Lu, H.; Yuan, M.; Fang, B.; Wang, J.; Guo, Y. Wormlike Micelles in Mixed Amino Acid-Based Anionic Surfactant and Zwitterionic Surfactant Systems. *J. Surfactants Deterg.* **2015**, *18*, 589−596.
(41) Förster, S.; Konrad, M.; Lindner, P. Shear Thinning and Orientational Ordering of Wormlike Micelles. *Phys. Rev. Lett.* **2005**, *94*, 017803.
(42) Fan, H.; Yan, Y.; Li, Z.; Xu, Y.; Jiang, L.; Xu, L.; Zhang, B.; Huang, J. General rules for the scaling behavior of linear wormlike micelles formed in catanionic surfactant systems. *J. Colloid Interface Sci.* **2010**, *348*, 491−497.

(43) Vu, T.; Koenig, P.; Weaver, M.; Hutton, H. D.; Kasting, G. B. Effects of cationic counterions and surfactant on viscosity of an amino acid-based surfactant system. *Colloids Surf., A* **2021**, *626*, 127040.
(44) Varade, D.; Rodríguez-Abreu, C.; Shrestha, L. K.; Aramaki, K. Wormlike Micelles in Mixed Surfactant Systems: Effect of Cosolvents. *J. Phys. Chem. B* **2007**, *111*, 10438−10447.
(45) Rogers, S. A.; Calabrese, M. A.; Wagner, N. J. Rheology of branched wormlike micelles. *Curr. Opin. Colloid Interface Sci.* **2014**, *19*, 530−535.
(46) Sakai, K.; Nomura, K.; Shrestha, R. G.; Endo, T.; Sakamoto, K.; Sakai, H.; Abe, M. Wormlike Micelle Formation by Acylglutamic Acid with Alkylamines. *Langmuir* **2012**, *28*, 17617−17622.
(47) Zhang, D.; Sun, Y.; Deng, Q.; Qi, X.; Sun, H.; Li, Y. Study of the environmental responsiveness of amino acid-based surfactant sodium lauroylglutamate and its foam characteristics. *Colloids Surf., A* **2016**, *504*, 384−392.
(48) Shrestha, R. G.; Shrestha, L. K.; Aramaki, K. Wormlike micelles in mixed amino acid-based anionic/nonionic surfactant systems. *J. Colloid Interface Sci.* **2008**, *322*, 596−604.
(49) Liu, X.; Wu, K.; Song, W.; Lei, Q.; Zhang, H.; Pan, J.; Ge, X. Aqueous solution thickening of amino acid based surfactant by alkylpyrrolidone. *J. Surfactants Deterg.* **2022**, *25*, 7−15.

https://doi.org/10.1021/acsomega.3c05855
ACS Omega 2023, 8, 37511−37520